表 3

家系のうち、黄色で囲んだ13家系は、規模が比較的大きくphaseを決めることが可能であった家系。
phaseが決められなかった場合は「/」で両方のアレルを記載した。
青い枠で囲んだ領域は全ての家系の発症者に共通したハプロタイプを認めた領域である。この範囲内にpurstrophin-1遺伝子（Q9H7K4）が存在する。

表 4

Marker	most common haplotype	frequency in control (%)	P2	P4	P14	T2	T3	T4	T5	T6	T7	T12	T15	T19	T21	T25	T26	T28	T30	T37	T42	T43	T44	T46
D16S3043	1	25.0	1	1/6	7	5	8	1	1/8	1	1/5	5	1/7	n.e.	1/8	n.e.	n.e.	1	n.e.	1	n.e.	1/5	1/5	1
D16S3031	9	68.1	9	9	9	9	9	9	10	1	10	9	9/10	9	9	9	1/9	9	9	9	9	9	9	9
D16S3019	4	41.4	4	4	4	4	4	4/5	3/4	3/4	3/4	1/4	4	n.e.	4	n.e.	4/7	3/4	2/4	n.e.	3/4	3/4	3/4	1
CTATT01	1	32.4	1	2/4	1	1	1	1	1/4	1	1	1	1	1/3	n.e.	1/3	n.e.	1/3	n.e.	1	n.e.	1/2	1	0/3
TAGA02	4	10.3	4	6	4	4	4	4/6	4/6	4/5	4	2/4	4/5	n.e.	4/5	n.e.	4	4/5	4	3/4	n.e.	5/6	4/5	2/6
GGAA05	1	1.4	1	6	1	1	5	1	1	1	2	1	2/4	1/3	1/5	5	1/2	1/7	1/5	1/3	1/3	1/5	2/4	3/6
D16S397	1	47.1	n.e.	1/2	1	1	1	0/4	1/2	1/3	1/3	2/3	1	n.e.	1	n.e.	n.e.	1/4	-3/0	-3/1	n.e.	-3/1	1	-3/1
GGAA10	3	13.2	3	3	3	3	4	3/5	3	3	3	3	3/6	2/3	2/4	3/7	3/5	3/8	4/6	3	3/6	3/5	3/7	3/7
GATA01	2	44.1	2	2/3	2	2	2	3	3	3	2	2	1/2	2/3	1/3	3/4	1/3	1/3	1	2	3	1/3	2/3	2/3
D16S421	3	75.7	3	3	3	3	3	3	3	3	3	3	3	3	3	3	3	3	3	3	3/4	3	3	3
puratrophin-1 (C/T)	T	0.0	T	T	T	T	T	T	T	T/C	T/C	T/C	T/C	T/C	T/C	T/C	T/C	T/C	T/C	T/C	T/C	T/C	T/C	T/C
TA001	1	23.8	1	1	1	1	1	1	1	1	1	1	1	1/9	1/7	2/8	1/6	1/10	1/9	1/9	1	1/9	1/9	1/5
GA001	4	0.1	4	4	4	4	4	4	4	4/7	4/7	4	4	1/4	4/8	4/5	4/7	4/7	4/6	4/11	4/5	4/7	4/6	4/7
17msm	2	8.3	2	2	2	2	2	2	2	2	2	5	2	2/5	2/5	2/4	2/4	2/4	2/4	2/5	2/4	2/4	4/6	2/4
D16S3107	7	13.9	7	7	7	7	7	7	6	7	7	7	5	6	5/6	3/7	6/10	6	7	5/7	3/7	6/7	4/7	6/7
GGAA01	6	18.8	6	6	6	6	6	6	6	6	6	6	1/6	3/6	2/6	2/6	4/6	6/7	6	6	6	6/7	6/7	5/6
CTTT01	8	28.2	8	8	8	8	9/10	8	5	9	8	10	8	9/10	3/9	9/10	8/10	8	8/11	6/9	8/15	9/10	1/7	3/8
GT01	6	15.8	6	6	6	6	6	6	6	6	6	4	6	2/6	1/6	4/6	4/6	2/6	5/6	4/6	6	3/6	3/4	4/6
D16S3095	1	9.7	2	3	1	0	1	1	2	3	2	1/2	1	1	1/2	1/2	1/2	1/3	1	1	1/2	1/3	2	1
D16S512	1	32.3	n.e.	2/4	1	4	1/5	4	2/4	1/5	1/5	1/5	4	n.e.	4/5	n.e.	n.e.	5	1	1/2	n.e.	2/4	4	4/5

■ は、共通するハプロタイプ（common haplotype）から2つ以上アレルが異なる場合。

▨ は、共通するハプロタイプ（common haplotype）から1つだけアレルが異なる場合。

表5

SNP	position on Chr 16	SNP change on 16q-ADCA	frequency in control (%)	P4	P14	T2	T3	T4	T5	T6	T7	T12	T15	T21	T28	T37	T43	T44	T46	U09
SNP01	64,972,150	A → G	27.8	G/A	G/A	G	G/A	G/A	G	G	G/A	G	G/A	G/A	G/A	G	G/A	G	A	G/A
SNP02	64,977,170	A → C	22.2	C/A	C/A	C	C/A	C/A	C	C	C/A	C	C/A	C/A	C/A	C	C/A	C/A	A	C/A
SNP03	64,977,733	T → C	30.0	C/T	C/T	C	C/T	C/T	C	C	C/T	C	C/T	C/T	C/T	C	C/T	C	T	C/T
SNP04	64,982,678	C → T	27.8	T/C	T/C	T	T	T/C	T	T	T/C	T	T/C	T/C	T	T	T/C	T	C	C/T
SNP05	65,049,292	G → A	0.0	A/G	A/G	A	A/G	A/G	A/G	A/G	A/G	A/G	A/G	A/G	A/G	A/G	A/G	A/G	A/G	A/G
SNP06	65,337,827	A → G	0.0	G/A	G/A	G	G/A	G/A	G/A	G/A	G/A	G/A	G/A	G/A	G/A	G/A	G/A	G/A	G/A	G/A
SNP07	65,449,825	C → T	56.3	T	T	T/C	T/C	T	T	T/C	T/C	T	T	T/C	T/C	T/C	T	T/C	T/C	T/C
SNP08	65,451,833	T → A	45.5	A	A	A/T	A/T	A	A	A/T	A/T	A	A	A/T	A/T	A/T	A	A/T	A/T	A
SNP09	65,457,741	T → A	42.4	A	A	A/T	A/T	A	A	A/T	A/T	A	A	A/T	A/T	A/T	A	A/T	A/T	A
SNP10	65,458,302	T → C	45.5	C	C	C	C/T	C/T	C	C	C/T	C/T	C	C	C/T	C/T	C/T	C/T	C/T	C
SNP11	65,669,454	T → C	30.3	C	C/T	C	C/T	C/T	C/T	C	C/T	C	C	C/T	C/T	C/T	C/T	C	C/T	C/T
SNP12	65,771,917	G → A	18.2	A	A/G	A	A/G	A/G	A/G	A/G	A/G	A/G	A	A/G	A/G	A/G	A/G	A	A/G	A/G
SNP13	65,793,152	C → T	8.7	T	C/T	T	C/T	C/T	C/T	C/T	C/T	C/T	C/T	C/T	C/T	C/T	T	C/T	C/T	C/T
puratrophin-1 (C/T)	65,871,434	C → T	0.0	T	T	T	T	T	T	T/C	T/C	T/C	T/C	T/C	T/C	T/C	T/C	T/C	T/C	C

研究成果の刊行に関する一覧表

原著論文

著者名	論文題目名	雑誌名	巻：頁，発行西暦年号
Ishikawa K., Toru S., Tsunemi T., Li M., Kobayashi K., Yokota T., Amino T., Owada K., Fujigasaki H., Sakamoto M., Tomimitsu H., Takashima M., Kumagai J., Noguchi Y., Kawashima Y., Ohkoshi N., Ishida G., Gomyoda M., Yoshida M., Hashizume Y., Saito Y., Murayama S., Yamanouchi H., Mizutani T., Kondo I., Toda T., Mizusawa H.	An autosomal dominant cerebellar ataxia linked to chromosome 16q22.1 is associated with a single-nucleotide substitution in the 5' untranslated region of the gene encoding a protein with spectrin repeat and Rho guanine-nucleotide exchange-factor domain.	Am J Hum Genet	77: 280-296, 2005.
Owada K., Ishikawa K., Toru S., Ishida G., Gomyoda M., Tao O., Noguchi Y., Kitamura K., Kondo I., Noguchi E., Arinami T., Mizusawa H.	A clinical, genetic, and neuropathologic study in a family with 16q-linked ADCA type III.	Neurology	65: 629-632, 2005.
Toru S., Yokota T., Tomimitsu H., Kanouchi T., Yamada M., Mizusawa H.	Somatosensory-evoked cortical potential during attacks of paroxysmal dysesthesia in multiple sclerosis.	Euro J Neurol	12: 233-234, 2005.
Amino T., Orimo S., Itoh Y., Takahashi A., Uchihara T., Mizusawa H.	Profound cardiac sympathetic denervation occurs in Parkinson disease.	Brain Pathol	15: 29-34, 2005.
Kubodera T., Yokota T., Ishikawa K., Mizusawa H.	New RNAi Strategy for Selective Suppression of Mutant Allele in Polyglutamine Disease.	Oligonucleotides	15: 298-302, 2005.
Ishikawa K., Mizusawa H.	On autosomal dominant cerebellar ataxia (ADCA) other than polyglutamine diseases, with special reference to chromosome 16q22.1-linked ADCA.	Neuropathology	26: 352-360, 2006.

43

次ページにつづく

原著論文（つづき）

著者	論文タイトル	雑誌	巻・頁
Ouyang Y., Sakoe K., Shimazaki H., Namekawa M., Ogawa T., Ando Y., Kawakami T., Kaneko J., Hasegawa Y., Yoshizawa K., Amino T., Ishikawa K., Mizusawa H., Nakano I., Takiyama Y.	16q-linked autosomal dominant cerebellar ataxia: A clinical and genetic study.	Journal of the Neurological Sciences	247: 180-186, 2006.
Ohata T., Yoshida K., Sakai H., Hamanoue H., Mizuguchi T., Shimizu Y., Okano T., Takada F., Ishikawa K., Mizusawa H., Yoshiura K., Fukushima Y., Ikeda S., Matsumoto N.	A -16C>T substitution in the 5' UTR of the puratrophin-1 gene is prevalent in autosomal dominant cerebellar ataxia in Nagano.	Journal of Human Genetics	51: 461-466, 2006.
Uchihara T., Takeda Y., Kobayashi T., Kasuga T., Ishikawa K., Kirei K., Mizusawa H., Endo T., Hirokawa K., Kuroiwa T.	Unexpected clinicopathological phenotype linked to small elongation of CAG repeat in SCA1 gene.	Journal of Neurology	253: 396-398, 2006.
Ienaga Y., Mitoma H., Kubota K., Morita S., Mizusawa H.	Dynamic imbalance in gait ataxia. Characteristics of plantar pressure measurements.	Journal of the Neurological Sciences	246: 53-57, 2006.
Amino T., Ishikawa K., Toru S, Ishiguro T., Sato N, Tsunemi T., Murata M, Kobayashi K, Inazawa J, Toda T, Mizusawa H.	Redefining the disease locus of 16q22.1-linked autosomal dominant cerebellar ataxia.	Journal of Human Genetics	52(8):643-9, 2007. Epub 2007 Jul 5.
Lin JX, Ishikawa K, Sakamoto M, Tsunemi T, Ishiguro T, Amino T, Toru S, Kondo I, Mizusawa H.	Direct and accurate measurement of CAG repeat configuration in the ataxin-1 (ATXN-1) gene by "dual-fluorescence labeled PCR-restriction fragment length analysis".	Journal of Human Genetics	53(4): 287-95, 2008. Epub 2008 Feb 27.
Li Y, Yokota T, Gama V, Yoshida T, Gomez JA, Ishikawa K, Sasaguri H, Cohen HY, Sinclair DA, Mizusawa H, Matsuyama S.	Bax-inhibiting peptide protects cells from polyglutamine toxicity caused by Ku70 acetylation.	Cell Death and Differentiation	14(12): 2058-67, 2007. Epub 2007 Sep21.

44

研究成果の刊行に関する一覧表

書籍

著者名	題目	書籍名、編集者	頁、発行西暦年号、出版社
Ishikawa K., Mizusawa H.	Spinocerebellar ataxia type 6.	Genetic Instabilities and Neurologic Diseases. 2nd Edition. Editors: Robert D. Wells & Tetsuo Ashizawa	Chapter 25, p379-385, 2006, Academic Press.
Ishikawa K., Flanigan K.M., Mizusawa H.	Chromosome 16q22.1-linked autosomal dominant cerebellar ataxia and spinocerebellar ataxia type 4, the two clinically distinct ataxias linked to the same locus.	Recent Advances in Spinocerebellar degenerations and Spastic Paraplegia. Editors: Nishizawa Masatoyo and Yoshihisa Takiyama.	Chapter 5, p57-68, 2008. Research Signpost Press, India.

総説

著者名	論文題目名	雑誌名	巻：頁、発行西暦年号
石川欽也, 高橋博樹, 水澤英洋.	脊髄小脳失調症6型 (SCA6) におけるめまい.	神経研究の進歩	49: 237-244, 2005.
石川欽也, 水澤英洋.	脊髄小脳変性症と痙性対麻痺.	ゲノム医学	5: 267-274, 2005.
石川欽也, 水澤英洋.	ポリグルタミン病.	ゲノム医学	5: 311-316, 2005.
坂本昌己, 水澤英洋.	小脳とその障害 −update 小脳の疾患と治療 優性遺伝性脊髄小脳変性症	Clinical Neuroscience	23: 1430-1432, 2005.
常深泰司, 水澤英洋.	ポリグルタミン病 −脊髄小脳失調症6型を中心に−. イオンチャネル最前線update.	別冊 医学のあゆみ.	227-231, 2005.
石川欽也, 融 衆太, 水澤英洋.	特集 脊髄小脳変性症の最近の進歩 「第16番染色体長腕に連鎖する優性遺伝性脊髄小脳変性症」	神経研究の進歩	50(3): 355-362, 2006.
石川欽也.	悪性腫瘍に関連した神経障害「小脳障害」	Clinical Neuroscience	24 (1): 70-72, 2006.
石川欽也, 水澤英洋.	第16番染色体長腕連鎖型脊髄小脳変性症	Clinical Neuroscience	25 (7):738-739, 2007.

研究成果の刊行に関する一覧表

An Autosomal Dominant Cerebellar Ataxia Linked to Chromosome 16q22.1 Is Associated with a Single-Nucleotide Substitution in the 5′ Untranslated Region of the Gene Encoding a Protein with Spectrin Repeat and Rho Guanine-Nucleotide Exchange-Factor Domains

Kinya Ishikawa,[1,*] Shuta Toru,[1,*] Taiji Tsunemi,[1] Mingshun Li,[1] Kazuhiro Kobayashi,[8]
Takanori Yokota,[1] Takeshi Amino,[1] Kiyoshi Owada,[1] Hiroto Fujigasaki,[1] Masaki Sakamoto,[1]
Hiroyuki Tomimitsu,[1] Minoru Takashima,[1] Jiro Kumagai,[2] Yoshihiro Noguchi,[3]
Yoshiyuki Kawashima,[3] Norio Ohkoshi,[9] Gen Ishida,[10] Manabu Gomyoda,[11] Mari Yoshida,[12]
Yoshio Hashizume,[12] Yuko Saito,[5] Shigeo Murayama,[5] Hiroshi Yamanouchi,[6]
Toshio Mizutani,[7] Ikuko Kondo,[13] Tatsushi Toda,[8] and Hidehiro Mizusawa[1,4]

Departments of [1]Neurology and Neurological Science, [2]Pathology, and [3]Audiovestibular Science, Graduate School, and [4]The 21st Century Center of Excellence Program on Brain Integration and Its Disorders, Tokyo Medical and Dental University, [5]Department of Neuropathology, Tokyo Metropolitan Institute of Gerontology, [6]Department of Neurology, Tokyo Metropolitan Geriatric Hospital, and [7]Department of Pathology, Tokyo Metropolitan Neurological Hospital, Tokyo; [8]Division of Functional Genomics, Department of Post-Genomics and Diseases, Course of Advanced Medicine, Osaka University Graduate School of Medicine, Osaka, Japan; [9]Department of Neurology, Institute of Clinical Medicine, University of Tsukuba, Tsukuba, Japan; Departments of [10]Neurology and [11]Clinical Laboratory, National Matsue Hospital, Matsue, Japan; [12]Department of Neuropathology, Institute of Medical Science of Aging, Aichi Medical University, Aichi, Japan; and [13]Department of Medical Genetics, Ehime University School of Medicine, Ehime, Japan

Autosomal dominant cerebellar ataxia (ADCA) is a group of heterogeneous neurodegenerative disorders. By positional cloning, we have identified the gene strongly associated with a form of degenerative ataxia (chromosome 16q22.1–linked ADCA) that clinically shows progressive pure cerebellar ataxia. Detailed examination by use of audiogram suggested that sensorineural hearing impairment may be associated with ataxia in our families. After restricting the candidate region in chromosome 16q22.1 by haplotype analysis, we found that all patients from 52 unrelated Japanese families harbor a heterozygous C→T single-nucleotide substitution, 16 nt upstream of the putative translation initiation site of the gene for a hypothetical protein DKFZP434I216, which we have called "puratrophin-1" (Purkinje cell atrophy associated protein-1). The full-length *puratrophin-1* mRNA had an open reading frame of 3,576 nt, predicted to contain important domains, including the spectrin repeat and the guanine-nucleotide exchange factor (GEF) for Rho GTPases, followed by the Dbl-homologous domain, which indicates the role of puratrophin-1 in intracellular signaling and actin dynamics at the Golgi apparatus. Puratrophin-1—normally expressed in a wide range of cells, including epithelial hair cells in the cochlea—was aggregated in Purkinje cells of the chromosome 16q22.1–linked ADCA brains. Consistent with the protein prediction data of puratrophin-1, the Golgi-apparatus membrane protein and spectrin also formed aggregates in Purkinje cells. The present study highlights the importance of the 5′ untranslated region (UTR) in identification of genes of human disease, suggests that a single-nucleotide substitution in the 5′ UTR could be associated with protein aggregation, and indicates that the GEF protein is associated with cerebellar degeneration in humans.

Introduction

Autosomal dominant cerebellar ataxia (ADCA) is a clinical entity of heterogeneous neurodegenerative diseases

that show dominantly inherited, progressive cerebellar ataxia that can be variably associated with other neurological and systemic features (Harding 1982). Circumscribed groups of neurons in the cerebellum, brainstem, basal ganglia, or spinal cord are selectively involved in different combinations and to varying extents among diseases (Graham and Lantos 2002). ADCA is now classified by the responsible mutations or gene loci. To date, 24 subtypes have been identified: spinocerebellar ataxia type (SCA) 1, 2, 3 (or, Machado-Joseph disease [MJD]), 4–8, 10–19/22, 21, 23, 25, 26; dentatorubral and pallidoluysian atrophy (DRPLA); and ADCA with mutation in fibroblast growth factor (FGF) 14 (Stevanin et

al. 2000, 2004; Margolis 2002; van Swieten et al. 2003; Yu et al. 2005). Among these, mutations in SCA1, SCA2, SCA3/MJD, SCA6, SCA7, SCA17, and DRPLA have been identified as the expansion of a trinucleotide (CAG) repeat that encodes the polyglutamine tract, uniformly causing aggregation of polyglutamine-containing causative protein (Ross and Poirier 2004). Expansion of noncoding trinucleotide (CAG or CTG) or pentanucleotide (ATTCT) repeats are involved in SCA8, SCA10, and SCA12 (Holmes et al. 1999; Koob et al. 1999; Matsuura et al. 2000). Very few families are affected by missense mutations in the protein kinase Cγ (PKCγ) (SCA14 [see Chen et al. 2003]) and *FGF14* genes (ADCA with *FGF14* mutation [see van Swieten et al. 2003]). However, genes or even their loci remain unidentified for >20%–40% of families with ADCA (Sasaki et al. 2003).

We had previously mapped mutations in six Japanese families with ADCA to a 10-cM interval in human chromosome 16q13.1-q22.1, identifying 16q-linked ADCA type III, or spinocerebellar ataxia 4 (SCA4 [MIM 600223]) (Ishikawa et al. 2000). Clinically, our families show cerebellar ataxia without obvious evidence of extracerebellar neurological dysfunction (i.e., "pure cerebellar ataxia," or "ADCA type III") (Harding 1982; Ishikawa et al. 2000). The average age at onset of ataxia was >55 years (Ishikawa et al. 1997), which suggests that this disease shows the oldest age at onset among ADCA types with assigned loci. Another important clinical feature of this disease is that a substantial number of patients show progressive sensorineural hearing impairment (Owada et al., in press). Since the hearing impairment can be very mild and of later onset, presence of hearing impairment can be easily overlooked. However, this finding may indicate that the mutated gene could cause hearing impairment as well as ataxia. In this sense, it would be more appropriate to use the term "chromosome 16q22.1–linked ADCA" instead of "ADCA type III" to describe our families. Neuropathological examination showed peculiar degeneration of Purkinje cells that was not described in other degenerative ataxias (Owada et al., in press). Many Purkinje cells undergo shrinkage and are surrounded by amorphous materials composed of Purkinje-cell somato-dendritic sprouts and an increased number of presynaptic terminals. These findings may indicate that certain proteins involved in the cytoskeleton of Purkinje cells are disturbed in chromosome 16q22.1–linked ADCA.

Chromosome 16q22.1–linked ADCA has been assigned to the same locus as another ADCA, SCA4 (Flanigan et al. 1996; Hellenbroich et al. 2003). Although SCA4 and chromosome 16q22.1–linked ADCA may be allelic, SCA4 is clinically distinct from chromosome 16q22.1–linked ADCA, because SCA4 shows prominent sensory axonal neuropathy and pyramidal tract signs, with an age at onset earlier than that of chromo-

some 16q22.1–linked ADCA (Flanigan et al. 1996; Hellenbroich et al. 2003). Several groups, including ours, have refined the loci of SCA4/chromosome 16q22.1–linked ADCA and have, so far, excluded repeat expansions as mutations (Hellenbroich et al. 2003; Li et al. 2003; Hirano et al. 2004). The minimum candidate region of SCA4 and chromosome 16q22.1–linked ADCA is set at the region between markers *D16S3031* and *D16S3095*. A strong founder effect has been observed for chromosome 16q22.1–linked ADCA (Li et al. 2003), which indicates the need to recruit a large number of families to narrow the critical region.

To discover the causative gene of chromosome 16q22.1–linked ADCA, we embarked on a positional cloning study by recruiting 52 families from diverse regions of Japan. Here, we describe the identification of a strong association between a single-nucleotide change and chromosome 16q22.1–linked ADCA and show the consequence of this genetic change on mRNA and protein levels. The data presented here also suggest that a single-nucleotide change in the 5′ UTR could be associated with aggregation of the gene product.

Patients, Material, and Methods

Recruitment of Families with Chromosome 16q22.1–Linked ADCA

We attempted to include families clinically diagnosed with late-onset ADCA type III from a wide region of Japan. Fifty-two families, including 109 affected individuals and 48 at-risk individuals, were ultimately recruited. These families originated from seven of eight districts of Japan (Hokkaido, Tohoku, Kanto, Chu-bu, Kinki, Chu-goku, and Kyu-shu), which indicates that their origins are widespread. Clinical features of these patients were consistent with those of families described elsewhere (Ishikawa et al. 1997, 2000; Li et al. 2003).

Detailed neuro-otological examinations, including pure-tone audiometry, were performed on 13 families at the Departments of Neurology and Otolaryngology, Tokyo Medical and Dental University. Progressive hearing impairment was assessed when the pure-tone average calculated from thresholds at the frequencies of 0.5, 1, and 2 kHz was more severe than the mean +2 SD of age-matched normal Japanese population (Tsuiki et al. 2002). By that criterion, 6 (42.9%) of 14 families had a hearing impairment other than age-related hearing loss. When we used the recommendations for the description of genetic and audiological data composed by the GENDEAG study group (see The Hereditary Hearing Loss Homepage), all of the patients with the hearing impairment were confirmed to have bilateral sensorineural hearing loss of mild-to-moderate severity. The audiometric configurations of these patients include mid-fre-

quency U-shaped, flat, and high-frequency sloping. These data would suggest that the hearing impairment in our families is not a coincidence.

Preparation of DNA and RNA Samples

After informed consent was obtained, genomic DNA was extracted from peripheral-blood lymphocytes or lymphoblastoid cell lines by use of methods described elsewhere (Ishikawa et al. 1997). All families were excluded for SCA1, SCA2, SCA3/MJD, SCA6, SCA7, SCA8, SCA12, SCA14, SCA17, and DRPLA by testing mutations in the disease genes. For expression analysis on an RNA level, frozen cerebellar tissues of four brains affected with Alzheimer disease (AD) (age at death, range 65–85 years; duration of the disease, range 5–10 years) were used as controls. Clinically, these patients with AD showed a moderate-to-severe degree of dementia, as measured by the Clinical Dementia Rating (Hughes et al. 1982). Neuropathology in the cerebella of these patients showed only a few senile plaques without neuronal losses. For chromosome 16q22.1–linked ADCA, two patients were studied (ages at death, 74 and 78 years). Both control and 16q22.1-linked ADCA brains were obtained at autopsy, with the families' written consents approved by each institutional ethical committee. These brains were immediately frozen and stored at −80°C until use. Total RNA was extracted from frozen cerebellar tissues as described elsewhere (Ishikawa et al. 1999). Poly-A$^+$ RNA was selected from total RNA by NucleoTrap (Macherey-Nagel).

Restriction of Candidate Interval by Genotyping and Haplotype Analysis

Genotypes were determined for 23 informative markers, including five new markers we identified (*GGAA10, TTCC01, TA001, GA001,* and *AAT01* [GenBank accession numbers AB13610, AB13611, AB13612, AB197662, and AB13613, respectively]) (table 1). Standard PCR was performed in a final volume of 20 μl, containing 10 ng of genomic DNA, 3.4 pmol of each primer, 2.5 mM of dNTP, and 0.75 U of *Taq* polymerase (Takara). Thermal cycling was performed at 94°C for 5 min for initial denaturing, 30 cycles of denaturation (94°C for 30 s), annealing (55°C for 30 s), and extension (72°C for 30 s), followed by a final extension at 72°C for 5 min in an ABI GeneAmp PCR system 9700 (PE Applied Biosystems). The amplified product was separated in the Automated Laser Fluorescent DNA Sequencer II (Pharmacia Biotech), and genotypes were determined with Fragment Manager (Pharmacia Biotech) (Ishikawa et al. 1997). Allele frequencies in the general population were analyzed in 500 unrelated individuals without personal or family history of ataxia or other degenerative diseases.

Table 1

Microsatellite Markers and Primer Sequences

The table is available in its entirety in the online edition of *The American Journal of Human Genetics.*

Haplotypes of 16q22.1 markers were determined for 10 families (fig. 1) that were informative for determining the phase of alleles. The remaining 42 families were not sufficiently informative for determining the phase. Paucity of informative families was mainly due to the late age at onset of this disease. For these uninformative families, only combinations of genotypes were assessed, and the region of genotypes shared with the larger 10 families was compared.

Screening for Mutation in 21 Different Candidate Genes

Within the most critical interval, 21 genes or clusters of ESTs were retrieved from the Ensembl, UniGene, National Center for Biotechnology Information (NCBI), and Celera databases. Primers were designed to amplify individual exon and intron-exon boundaries for each gene, and genomic DNA was amplified by the aforementioned standard PCR protocol (primer sequences are available on request). Amplicons from controls and patients were first separated on 2% agarose gels, to determine by screening whether any aberrant bands were amplified from patient DNA samples. Residual solutions of PCR products were then purified with QIAquick PCR purification kit (Qiagen) and were directly sequenced using Applied Biosystems Model 377 or 3100 Automated Sequencer, as described elsewhere (Li et al. 2003). The mutation was analyzed by comparing sequenced data and annotated databases, with use of the software DNASIS (Hitachi). Genomic rearrangement was screened by Southern-blot analysis by use of cosmid clones for probe synthesis as described elsewhere (Kobayashi et al. 1998). In brief, cosmid clones, tandemly covering the chromosome 16q22.1–linked ADCA critical region, were generated by subcloning from the BAC contig (Li et al. 2003). Then, the radiolabeled (^{32}P) probe was generated from each cosmid clone. Genomic DNA extracted from lymphoblastoid cell lines of control individuals and patients with chromosome 16q22.1–linked ADCA was digested with a restriction enzyme and was subjected to Southern-blot analysis. To screen gene arrangement, analysis was performed with six different restriction enzymes (*Bam*HI, *Bgl*II, *Eco*RI, *Eco*RV, *Hind*III, and *Xba*I).

Twenty-one exons and 20 introns of the *puratrophin-1* gene, partially annotated as "*Q9H7K4*," were sequenced entirely. The genomic region between the *puratrophin-1* gene and *SLC9A5* was also screened (fig. 2).
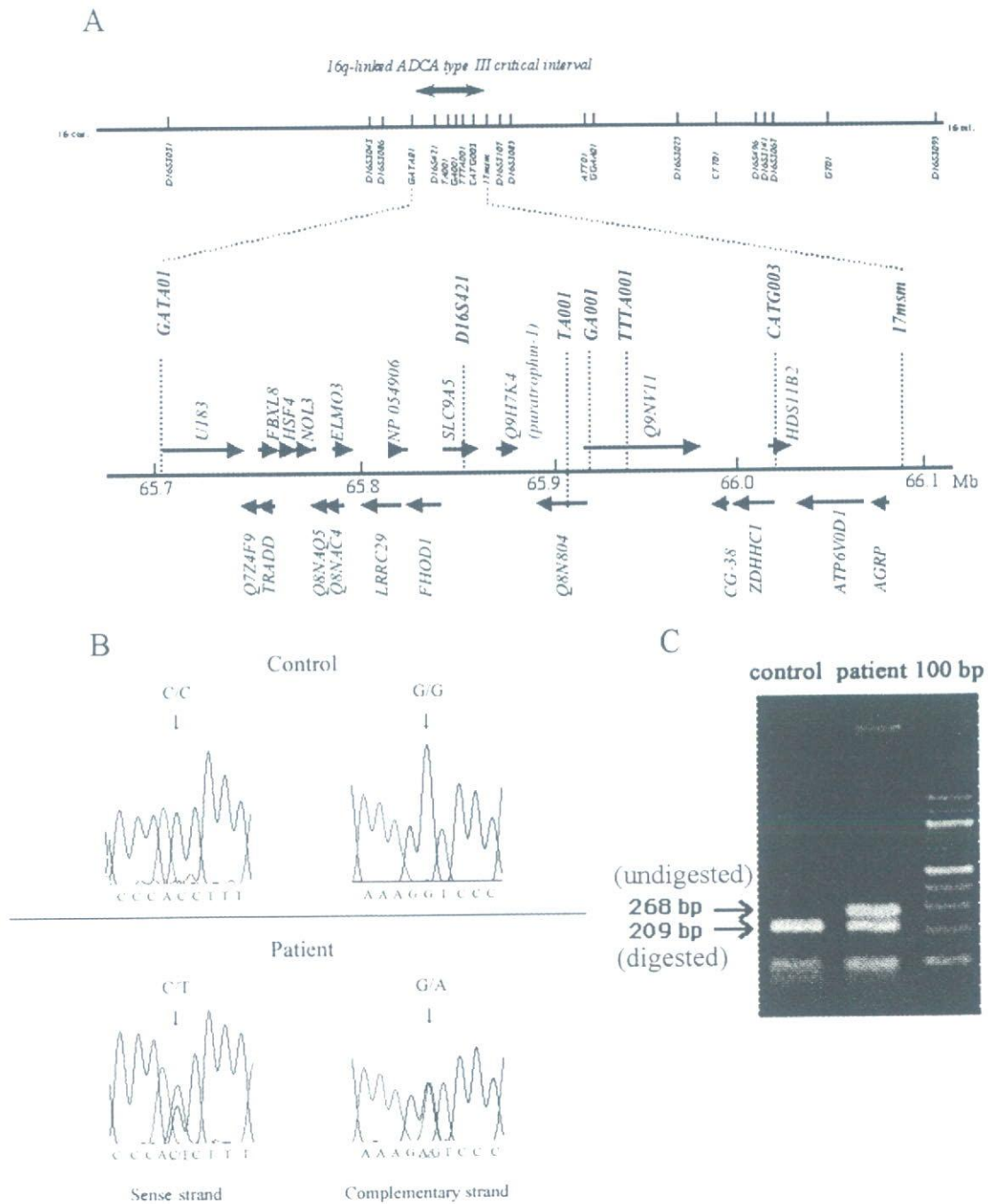
Figure 1 Haplotype analysis in the chromosome 16q22.1–linked ADCA critical locus. Ten families (P2, P4, P6, P12, P14, and T1–T5) large enough for haplotype analysis are indicated (yellow boxes at top). A founder haplotype "3-1-4-4-4" was seen in all patients for markers 16cen-D16S421-TA001-GA001-TTTA001-CATG003-16qter, between GATA01 and 17msm. Two alleles are shown (separated by a virgule [/]) for cases in which phase could not be determined. An asterisk (*) indicates that P values show significant linkage disequilibrium by Fisher's exact probability test. The specific C→T change in the puratrophin-1 gene lies within the founder chromosomal region.

Figure 2 Positional cloning of the chromosome 16q22.1–linked ADCA gene. A, Genetic and physical maps of the interval in chromosome 16q22.1, showing microsatellite markers used to refine the interval. Twenty-one genes and their direction of transcription (Ensembl) are shown. B, Nucleotide sequences of exon 1 flanking the C→T single-nucleotide change in control and patient DNA samples. The patient harbors a heterozygous C→T substitution on the sense strand. C, RFLP by digestion with *Eco*NI. PCR was performed with primers UK1-E1F1 and UK1-E1R1. Whereas the normal allele produces digested fragments of 209, 92, and 59 bp, the C→T change in the mutant allele disrupts one *Eco*NI site, producing fragments of 268 and 92 bp.

The C→T change in the 5' UTR was detected by amplifying genomic DNA with forward primer UK1-E1F1 (5'-CAGCGCGGTTCACACTGAGA-3') and reverse primer UK1-E1R1 (5'-GGCCCTTTCTGACAGGAC-TGA-3'), which yielded a specific product of 360 bp. This amplicon harbors two *Eco*NI sites, one of which is destroyed by the C→T change.

Expression Analysis of Puratrophin-1 mRNA by RT-PCR

To characterize *puratrophin-1* mRNA in the human brain, poly-A⁺RNA obtained from control human cerebellar tissues was reverse transcribed with SuperScript II (Stratagene), and the entire coding region was amplified with primers UKI-RT-025F (5'-TTCGCCTGCATTG-CCCACTGAG-3') and UK1-RT-005R (5'-CACACACA-TCAGAAAGGGTAGTCAAC-3'), which yielded a major product of 3,835 bp. To analyze alternative transcription, the PCR products were subcloned into pCR2.1-TOPO (Invitrogen), and 10 randomly selected clones from each brain mRNA (2 AD and 2 chromosome 16q22.1–linked ADCA cerebella) were sequenced and compared with partially annotated sequences (Q9H7K4, NCBI accession numbers BC054486 and AK024475). Rapid cloning of the 5' and 3' ends (5'- and 3'-RACE) was performed using Marathon-ready cDNA kit (Clontech [BD Biosciences]) as described elsewhere (Tsunemi et al. 2002). The entire 5' UTR was amplified with primers UK1-RT-493F (5'-TGAGACAGTCTCAGTCAGG-TCAC-3') and UK1-RT-021R (5'-GTGGGCACACAG-AAGCAGCACTGC-3'), was subcloned into pCR2.1-TOPO (Invitrogen), and was sequenced.

Expression of the *puratrophin-1* gene in various human tissues was studied by RT-PCR with use of primers UKI-RT-025F and UK1-RT-005R on human Multiple Tissue Panels I and II (Clontech [BD Bioscience]). Expression levels of *puratrophin-1* mRNA were compared among control and patient cerebellar cortices by RT-PCR with use of primers UK1-RT-BF001F (5'-TCA-CGGTTCCCCGCGGCTCG-3') and UK1-RT-BF019R (5'-GGTTGCATGGCCCTGAGAGTCTGG-3'), which yielded PCR products of 291, 419, and 505 bp, depending on alternative transcription. To compare *puratrophin-1* mRNA levels more precisely, real-time RT-PCR analysis was performed on four control (individuals with AD) and two chromosome 16q22.1–linked ADCA cerebella by use of TaqMan technique (Applied Biosystems) on Applied Biosystems 7700 Sequence Detection System. PCR was performed for total *puratrophin-1* mRNAs (i.e., full-length and short-form mRNAs [GenBank accession numbers AB197663 and AB197664, respectively]; definitions of these two isoforms are described in the "Results" section) with primers total-taq-F (5'-TGGAGAGATGAGTGTCAAGACTTTG-3') and total-taq-R (5'-AATGACTTGGGTCTGCCTTGG-3').

The short-form *puratrophin-1* mRNA was specifically assessed with primers short-taq-F (5'-ATGCCACCGAC-TGGAGATTT-3') and short-taq-R (5'-GCTGCCCTGT-AGCTCCTCAT-3'). The TaqMan probe for total *puratrophin-1* mRNA was 5'-FAM-CCAGATGCACGTTA-AGGACCCAGGTC-TAMRA-3', and that for short-form *puratrophin-1* mRNA was 5'-FAM-TCTCTGAC-CCTACTCAGGCTGAAGCCC-TAMRA-3'. The experiments were performed three times and were averaged. The level of *puratrophin-1* mRNA was assessed relative to the level of *G3PDH* mRNA amplified with primers supplied from the manufacturer (Applied Biosystems). Since the expression level of *G3PDH* mRNA was >1,000-fold higher than that of *puratrophin-1* mRNA, one control individual was chosen and the value of *puratrophin-1* mRNA:*G3PDH* mRNA ratio (designated "*puratrophin-1* mRNA/*G3PDH* mRNA index") was standardized as "1"; another three control individuals and two patients were compared relatively. The difference between the control and patient groups was statistically analyzed with the Mann-Whitney U test.

To see the effect of the C→T change in the 5' UTR of *puratrophin-1* gene on expression in vitro, the partial 5'-UTR fragment containing the mutation site was amplified with forward primers UK1-UF10-F2 (5'-CCG-GAATTCCAGGCCTGAATTGCAGTTC-3') and UK1-UF10-R2 (5'-CCAGGCATCCCTGAAACT-3') and was subcloned into the *Hind*III-*Nco*I sites of the luciferase assay vector, pGL3-Control Vector (Promega). The C→T mutation was then generated by site-directed mutagenesis (Stratagene). Three types of vectors (mock, empty pGL3-Control Vector; wild-type, pGL3 with normal *puratrophin-1* 5' UTR with allele C; and mutant, pGL3 with mutant *puratrophin-1* 5' UTR with allele T) were separately transfected with Renilla vector (Promega) into HEK293 cells to equalize the transfection efficiency. The transfection experiment was performed independently three times. Luciferase activity (F/R: fire-fly luciferase activity against Renilla activity) was assayed in accordance with the manufacturer's protocol and was statistically analyzed with the Mann-Whitney U test.

Generation of Rabbit Polyclonal Antibodies against Puratrophin-1

On the basis of the deduced amino acid sequence of "full-length" and "short-form" puratrophin-1, the secondary structure of each isoform was predicted, and five synthetic peptides were designed: polypeptide *FL01* (aa 1–13), N-MERPLENGDESPD-C; *FL02* (aa 421–432), N-MDKADELYDRVD-C; *FL03* (aa 570–583), N-EEG-QRVLAELEQER-C; *FL04* (aa 991–1003), N-RFEIW-FRRRKARD-C; and *SV01* (aa 13–26), N-REVWEGN-GDAWRDE-C. The polypeptide FL01 lies at the amino terminus of the puratrophin-1 (fig. 3). Therefore, the
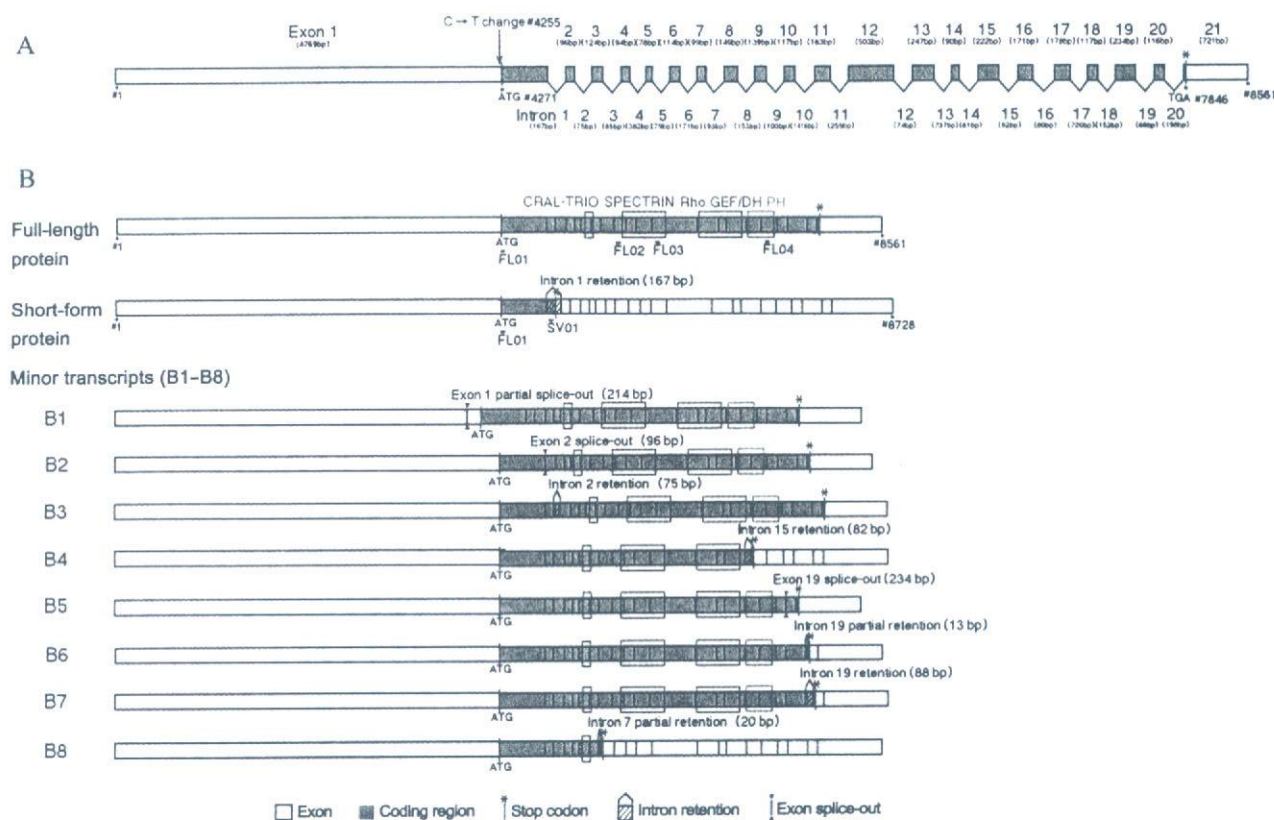
Figure 3 Genomic and mRNA structure of the *puratrophin-1* gene. *A,* Intron-exon structure of *puratrophin-1.* Exons are shown as vertical bars, and coding regions are shown in red. The C→T change at nt 4255 (or, 16 nt upstream of the translation initiation codon) is indicated. Nucleotide numbers (indicated by a number sign [#]) are counted from the 5′ end. *B, Puratrophin-1* mRNAs cloned from the human cerebellum. Major transcripts are full-length and short-form *puratrophin-1* mRNAs; minor transcripts (B1–B8) were also cloned. The CRL-TRIO, spectrin, Rho GEF/DH, and PH domains are indicated. Epitopes for five rabbit anti–puratrophin-1 antibodies (FL01–FL04 and SV01) are also mapped. Antibodies FL02, FL03, and FL04 are designed to specifically detect full-length puratrophin-1, the antibody SV01 specifically detects short-form puratrophin-1, and the antibody FL01 detects both full-length and short-form puratrophin-1.

antibody Prtrphn1-Ab FL01 would detect both full-length and short-form puratrophin-1. The polypeptides FL02, FL03, and FL04 are specific for the full-length puratrophin-1 (fig. 3). Notably, FL03 is at the spectrin repeat motif. The polypeptide SV01 lies at the carboxyl-terminus of the short-form puratrophin-1. Therefore, the antibody Prtrphn1-Ab SV01 would specifically recognize the short-form puratrophin-1. Each antigen was immunized into rabbit, and polyclonal antibodies were obtained as described elsewhere (Ishikawa et al. 1999).

The specificity of Prtrhn1-Abs was assessed by detection of recombinant puratrophin-1 protein. For this purpose, an antisense-strand primer was designed to encode hemagglutinin A (HA) in-frame at the carboxyl-terminus of the puratrophin-1. By PCR, full-length *puratrophin-1* cDNA with the HA-coding nucleotide sequence at its 3′ end was generated and was then cloned into pcDNA1 expression vector (Invitrogen). The puratrophin-1–HA fusion protein, transiently expressed in HEK293 cells,

was first immunoprecipitated with Prtrhn1-Abs and then was detected with rat monoclonal anti-HA High Affinity antibody (3F10 [Roche Mannheim]) (fig. 4). The fusion protein immunoprecipitated with preimmune sera was not detected with anti-HA antibody.

Specificity of Prtrphn1-Abs on immunohistochemistry was assessed by immunoabsorption test. Solutions containing Prtrphn1-Ab and different concentrations of antigen (synthetic peptide) (0, 0.01, 0.1, and 1 mg/

The figure is available in its entirety in the online edition of *The American Journal of Human Genetics.*

Figure 4 Immunoprecipitation of puratrophin-1–HA fusion protein and immunoabsorption test with antiserum against puratrophin-1. The legend is available in its entirety in the online edition of *The American Journal of Human Genetics.*

liter) were made. Sections were incubated overnight with these solutions as other immunohistochemical staining. Prtrphn1-Abs were completely absorbed by peptides of higher concentrations (fig. 4).

Immunohistochemical Analyses of Puratrophin-1, Golgi-Apparatus Protein G58K, and Spectrin in Control Mouse, Human, and 16q22.1-Linked ADCA Tissues

Five polyclonal antibodies against puratrophin-1 (Prtrphn1-Ab types *FL01*, *FL02*, *FL03*, *FL04*, and *SV01*) were used for immunohistochemistry. Mouse monoclonal antibody against the microtubule-binding peripheral Golgi-apparatus membrane protein G58K (Sigma) and the mouse monoclonal antibody for α- and β-spectrin (MAB372 [Chemicon International]) were also used for immunohistochemistry.

Formalin-fixed paraffin-embedded tissue sections were prepared. Examined tissues were C57BL/6J wild-type mouse tissue, including cochlea (1 d postnatal), normal-control human tissues (testis, pancreas, prostate gland, lung, liver, heart, kidney, and brain from three individuals who died with nonneurological diseases), disease-control human brains (AD [$n = 3$], SCA6 [$n = 2$], multiple-system atrophy [MSA] [$n = 3$], and SCA3/MJD [$n = 3$]), and three brains with chromosome 16q22.1–linked ADCA. Immunohistochemistry was performed as described elsewhere (Ishikawa et al. 1999). In brief, sections were incubated overnight with Prtrphn1-Abs (diluted 1:200 with PBS), G58K (diluted 1:400), or MAB372 (diluted 1:200) at 4°C, after which the primary antibody was serially detected with avidin-biotinylated peroxidase complex method (Vector), was developed with 3,3′-diaminobenzidine (DAB), and was counterstained with hematoxylin.

Results

Restriction of the Critical Interval to <600 kb within Human Chromosome 16q22.1

Haplotype reconstruction of 10 informative families revealed that all affected individuals in these families were segregated with the haplotype 3-1-4-4-4 for markers *16cen-D16S421-TA001-GA001-TTTA001-CATG003-16qter* lying between *GATA01* and *17msm* (fig. 1). Genotypes of all affected individuals in the remaining 42 families that were not informative enough for haplotype reconstruction were also consistent with the common haplotype. Particularly, a dinucleotide (GA) repeat marker *GA001* showed strong linkage disequilibrium: the allele 4 of GA001 was seen in all affected individuals in all families with chromosome 16q22.1–linked ADCA, whereas that allele was seen very rarely (frequency 0.1%) in 1,000 control chromosomes (fig. 1). Whereas only one common haplotype was seen between *GATA01*

and *17msm*, different alleles were seen for *GATA01* and other centromeric markers or for *17msm* and other telomeric markers (fig. 1). These results indicate that the gene for chromosome 16q22.1–linked ADCA is most likely to exist in the interval between *GATA01* and *17msm*. This region was within the previously refined intervals (Hellenbroich et al. 2003; Li et al. 2003) and was considered to be <600 kb in size in the database Ensembl.

Identification of a Single-Nucleotide Substitution in the 5′ UTR of the Gene Encoding Puratrophin-1 in the Critical Interval

Within the critical interval between *GATA01* and *17msm*, 21 different genes were identified (fig. 2A). We screened all 21 genes by direct sequencing of amplified genomic PCR products of all coding exons and flanking intronic sequences. Genomic Southern-blot analyses were also performed but did not detect any rearrangement (fig. 5).

We found that all patients with chromosome 16q22.1–linked ADCA harbored a heterozygous C→T single-nucleotide substitution at the position 16 nt upstream of the putative translation initiation codon of the gene *Q9H7K4*, encoding hypothetical protein DKFZP434I216 (NCBI accession number BC054486) (fig. 2B). All the at-risk individuals who had the founder haplotype between *GATA01* and *17msm* also harbored the C→T change. The ages of these individuals were below the maximum age at disease onset in their families, which indicates that they could be in presymptomatic stages. On the other hand, this C→T substitution was not seen in 500 healthy Japanese individuals (1,000 chromosomes), confirmed by *Eco*NI RFLP analysis (fig. 2C). All intronic sequences between the 21 exons and all the 8-kb sequences upstream of the *Q9H7K4* gene were also directly sequenced. Although there was a G→A SNP 44 nt upstream of the 3′ splice site of intron 9 of the *Q9H7K4* gene, the allele segregating with the disease was also seen in 75% of control chromosomes. As far as we examined, the C→T change at the position 16 nt upstream of the putative translation initiation codon of the gene *Q9H7K4* was the only specific change seen for patients with chromosome 16q22.1–linked ADCA. We renamed this protein "puratrophin-1," meaning <u>Pur</u>kinje cell <u>atrophy</u> associated

---

The figure is available in its entirety in the online edition of *The American Journal of Human Genetics*.

Figure 5   Southern-blot analysis. The legend is available in its entirety in the online edition of *The American Journal of Human Genetics*.
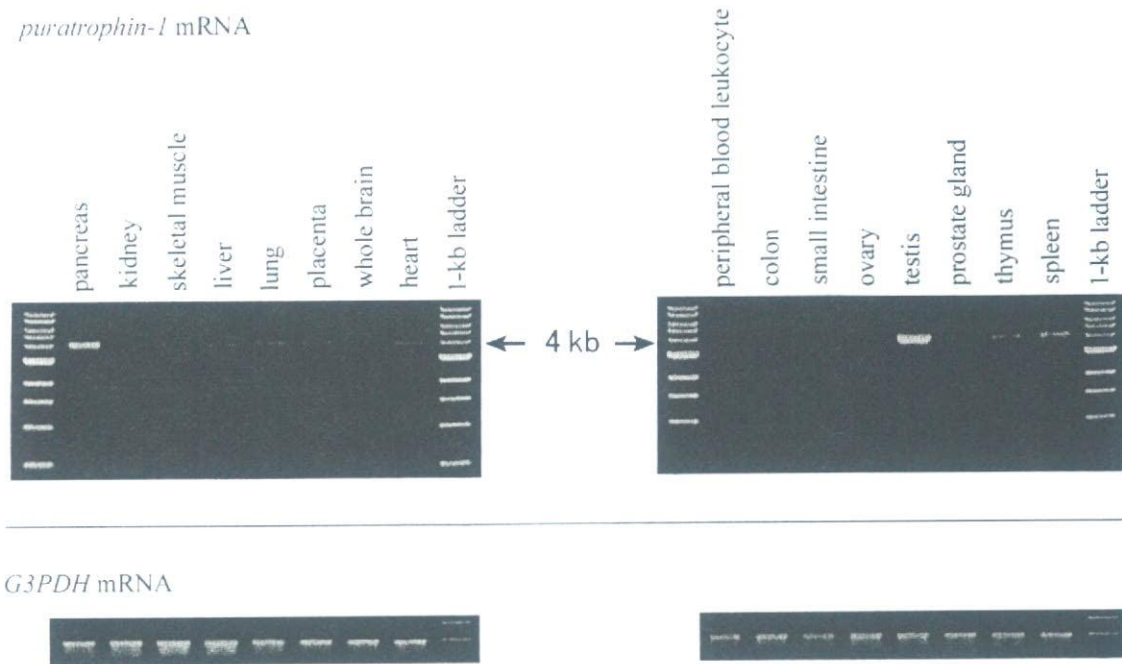
Figure 6 *Puratrophin-1* mRNA expression in various control human tissues. With this nonquantitative RT-PCR analysis, a relatively stronger expression was observed in the testis and pancreas, whereas mild or moderate expression was seen in the spleen, thymus, prostate gland, heart, placenta, lung, liver, and kidney. *Puratrophin-1* mRNA expression was low in the ovary, small intestine, colon, peripheral-blood leukocytes, whole brain, and skeletal muscle.

protein-1. (We reserved the nomenclature "ataxin-4" for families with original SCA4.)

Characterization of the Puratrophin-1 *Gene and Its Expression*

The *puratrophin-1* gene comprises 20 introns and 21 exons spanning a 13.7-kb genomic region (fig. 3A). RT-PCR and RACE experiments revealed that this gene is expressed in the human brain with an 8,561-nt mRNA and a single ORF of 3,576 nt (from nt 4,271 to nt 7,846) (fig. 3B). The first exon was 4,769 nt in length. This "full-length" transcript is predicted to encode a 134-kD protein, consisting of 1,192 aa, that contains four important domains: the cellular retinaldehyde-binding (CRAL)/triple function domain (TRIO) (at codons 304–338), the spectrin-repeat domain in the middle portion (at codons 447–601), the guanine-nucleotide exchange factor (GEF) for Rho/Rac/Cdc42-like GTPases followed by the Dbl-homologous (Rho GEF/DH) domain (at codons 733–907), and the pleckstrin-like homology (PH) domain (at codons 921–1027). The presence of these four domains suggests the role of puratrophin-1 in intracellular signaling and actin dynamics targeted to the Golgi apparatus (Godi et al. 1998; Fucini et al. 2000).

Besides the full-length *puratrophin-1* mRNA, we also found several alternative transcripts in human cerebellar cDNA (fig. 3B). The most common one had an unspliced intron 1 between exons 1 and 2 ("short-form" *puratrophin-1* mRNA). This intron retention produced a frameshift after exon 1 that resulted in a premature stop codon after 26 aa residues in intron 1. There were several other alternative transcripts (B1–B8 [fig. 3B]) in addition to full-length and short-form *puratrophin-1* mRNA. However, expression levels of these transcripts were considered lower than those of full-length or short-form *puratrophin-1* mRNA, as judged from cloning frequencies. *Puratrophin-1* mRNA was expressed in many tissues with various expression levels (fig. 6). The strongest expression was observed in the testis and pancreas, whereas its expression level was low in the "whole" brain. The expression was very weak on northern-blot analysis, even in the testis and pancreas (data available on request), which indicates that the expression of *puratrophin-1* mRNA was not abundant.

The Consequence of a C→T Change for Puratrophin-1 *mRNA Expression*

The consequence of the C→T change in the *puratrophin-1* gene was assessed by RT-PCR on frozen cerebellar tissues of two patients. No aberrant *puratrophin-1* mRNA was detected, which indicates that the mutation in the 5′ UTR does not affect alternative transcrip-
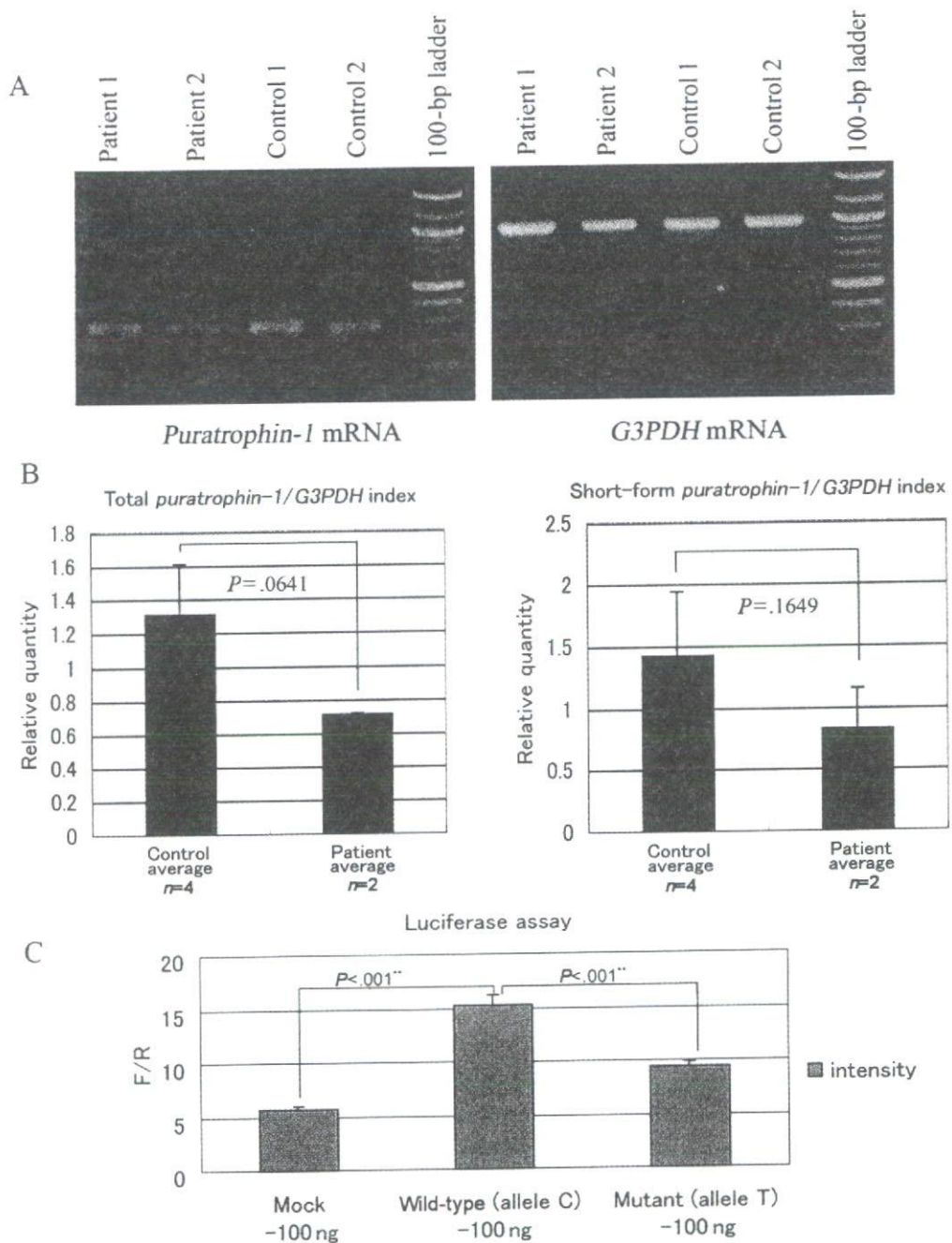
Figure 7 The consequence of a C→T change in the 5' UTR of *puratrophin-1* mRNA. *A*, The *puratrophin-1* mRNA level assessed relative to *G3PDH* mRNA levels. The *puratrophin-1* mRNA levels in the cerebella of individuals with chromosome 16q22.1–linked ADCA appear slightly decreased compared with levels in control individuals. *B*, Quantitative analysis of *puratrophin-1* mRNA, with the use of the TaqMan technique in cerebellar mRNAs of four control individuals (with AD) and of two individuals with chromosome 16q22.1–linked ADCA. Both total *puratrophin-1* mRNA (i.e., full-length and short-form mRNAs) and short-form *puratrophin-1* mRNAs tended to be reduced in cerebella of individuals with chromosome 16q22.1–linked ADCA, although the significance was not statistically proven ($P = .0641$ for total mRNA; $P = .1649$ for short-form mRNA). *C*, Histogram of in vivo luciferase assay. "F/R" denotes fire-fly luciferase activity versus Renilla activity. The wild-type construct with allele C increases luciferase expression compared with an empty vector (Mock), whereas the mutant construct with allele T demonstrates significantly reduced luciferase activity ($P < .001$).
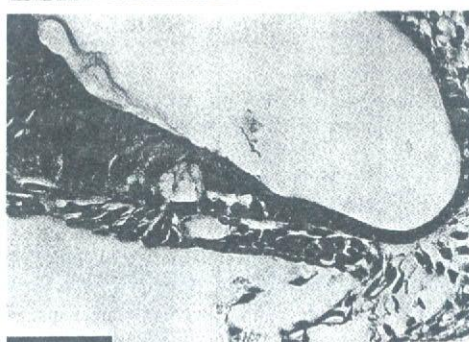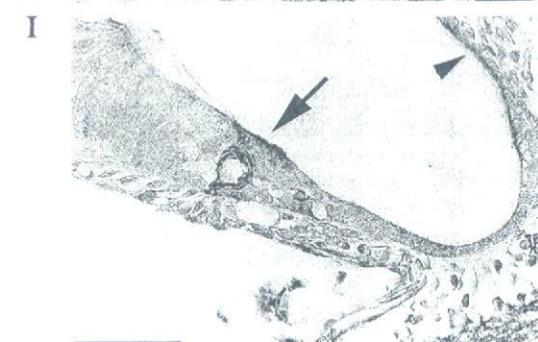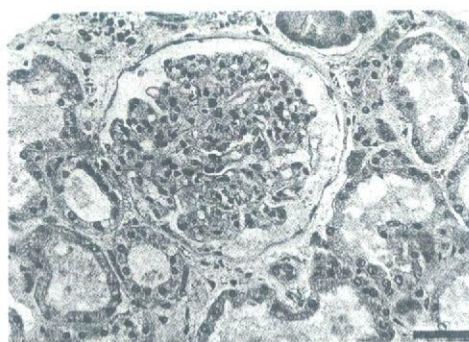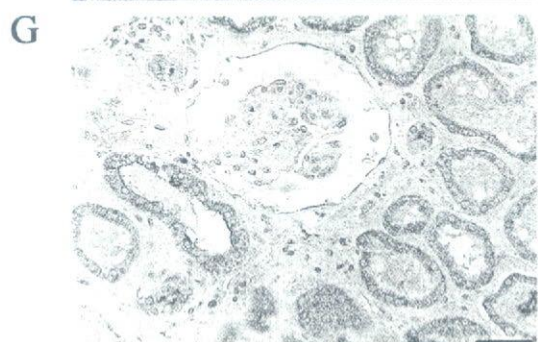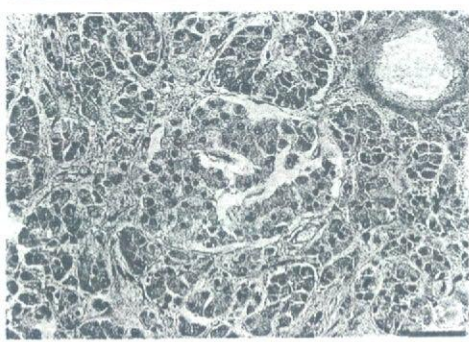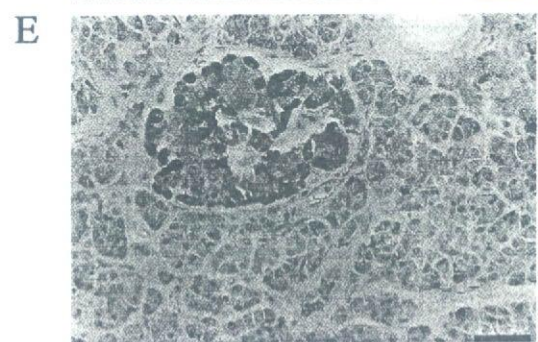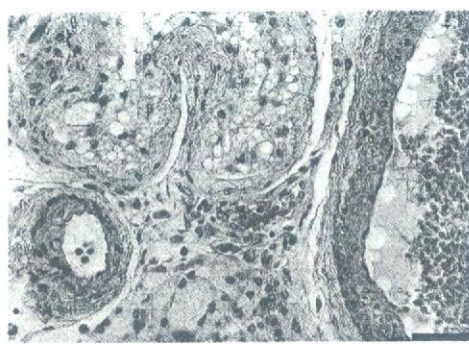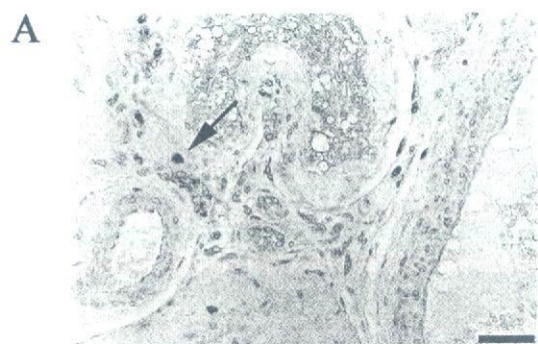
tion significantly. Instead, the expression level of *puratrophin-1* mRNA in the patient cerebella appeared slightly low compared with that in control cerebella (fig. 7A). On real-time RT-PCR analysis by TaqMan technique, the expression of *puratrophin-1* mRNA in the patient cerebella appeared lower than that in the control samples (fig. 7B). The tendency of reduction was seen for both total and short-form *puratrphin-1* mRNAs, although the significance was not proven statistically ($P = .0641$ for total *puratrophin-1* mRNA; $P = .1649$ for short-form *puratrophin-1* mRNA).

The in vitro study with *puratrophin-1* 5'-UTR sequences subcloned into luciferase expression vectors showed significantly reduced luciferase activity; the construct had mutant allele T, and the wild-type construct had allele C (fig. 7C). These data suggest that the C→T change in the *puratrophin-1* 5' UTR could lead to reduced mRNA expression.

Expression of Puratrophin-1 in Control Human and Mouse Tissues and in Brains of Patients with 16q22.1–Linked ADCA

We next examined puratrophin-1 expression by immunohistochemistry using rabbit polyclonal Prtrhn1-Abs. Puratrophin-1 expression was seen in many control human tissues and mouse cochlea (fig. 8). Interestingly, puratrophin-1 expression was commonly seen in epithelial cells, such as epithelial cells in the human testis and hair cells in the mouse cochlea. As far as we examined in human tissues, the strength of immunoreactivity correlated with the mRNA expression level revealed by RT-PCR experiments (fig. 6).

In control human brains, both full-length and short-form puratrophin-1 was expressed faithfully in various neurons but most strongly in Purkinje cells (fig. 9A). In chromosome 16q22.1–linked ADCA brains, a striking difference was noted: the presence of microscopic aggregates of puratrophin-1 in the cytoplasm of Purkinje cells (fig. 9B). These aggregates were detected with all Prtrhn1-Abs, which indicates that full-length puratrophin-1 and short-form puratrophin-1 were both involved in the aggregate. On the other hand, puratrophin-1 aggregates were not obvious in neurons other than Purkinje cells. The finding of puratrophin-1 aggregates was specific to chromosome 16q22.1–linked ADCA brains, since the aggregates were not seen in other dis-

eases showing degeneration of Purkinje cells, such as SCA6 or MSA.

We next examined the expression of G58K and of the α- and β-spectrin on control and chromosome 16q22.1–linked ADCA brains. Whereas G58K and spectrin were homogeneously stained in control brains (fig. 9C and 9E), these proteins both formed aggregation within the Purkinje cell of chromosome 16q22.1–linked ADCA brains (fig. 9D and 9F). This further suggests that formation of puratrophin-1 aggregates is abnormal and associates with disturbances of Golgi apparatus and spectrin.

Discussion

The single-nucleotide C→T substitution in the 5' UTR of the *puratrophin-1* gene is strongly associated with chromosome 16q22.1–linked ADCA, as evidenced by the following three points. First, this single-nucleotide change was the only specific difference detected in patients, as far as we screened all exons and intron-exon boundaries of the 21 annotated genes lying within the founder chromosome. The change completely segregated with the disease in 52 unrelated families that originated in all sections of Japan, whereas such a change was not seen in 1,000 control chromosomes. We also screened for genomic rearrangement by Southern-blot analysis, but we did not observe any changes. Second, the C→T change was not a mere polymorphism present in the founder chromosome, since it resulted in reduced expression in the in vitro luciferase assay. Consistently, tendency for reduction in mRNA expression was seen in the cerebellum of chromosome 16q22.1–linked ADCA. Third, puratrophin-1 was aggregated in the major target neuron (i.e., the Purkinje cell) of chromosome 16q22.1–linked ADCA. The Golgi-apparatus membrane protein (G58K) and spectrin, both important cytoskeletal proteins, were also aggregated. Since aggregation of mutated protein is a common feature of many neurodegenerative disorders (Ross and Poirier 2004), a single-nucleotide change in the 5' UTR in the *puratrophin-1* gene appears to be the mutation that causes chromosome 16q22.1–linked ADCA. Most mutations that cause ADCAs reside in genes encoding proteins whose functions are not well understood, except for the α1A-calcium channel (Ca$_v$2.1) for SCA6 (Zhuchenko et al. 1997), PKCγ for

Figure 8   Expression of puratrophin-1 in control human and mouse tissues. *A* and *B*, Human testis. *C* and *D*, Human prostate gland. *E* and *F*, Human pancreas. *G* and *H*, Human kidney. *I* and *J*, Mouse cochlea. *A*, *C*, *E*, *G*, and *I*, Immunohistochemical analysis with use of the polyclonal anti–puratrophin-1 antibody SV01. *B*, *D*, *F*, *H*, and *J*, Hematoxylin and eosin stain of the section adjacent to that shown in *A*, *C*, *E*, *G*, and *I*, respectively. Puratrophin-1 is expressed in many tissues, with varying strength. In particular, Leydig cells in the testis (*arrow* in *A*), epithelial cells in the prostate gland (*C*), and Langerhans islet in the pancreas (*E*) showed strong immunoreactivity. Immunoreactivity in the kidney was weak (*G*). Expression in the cochlea was particularly intense at the sensory hairlets (*arrow* in *I*). Hair cells of the stria vascularis also showed immunoreactivity (*arrowhead* in *I*). All scale bars = 50 μm.
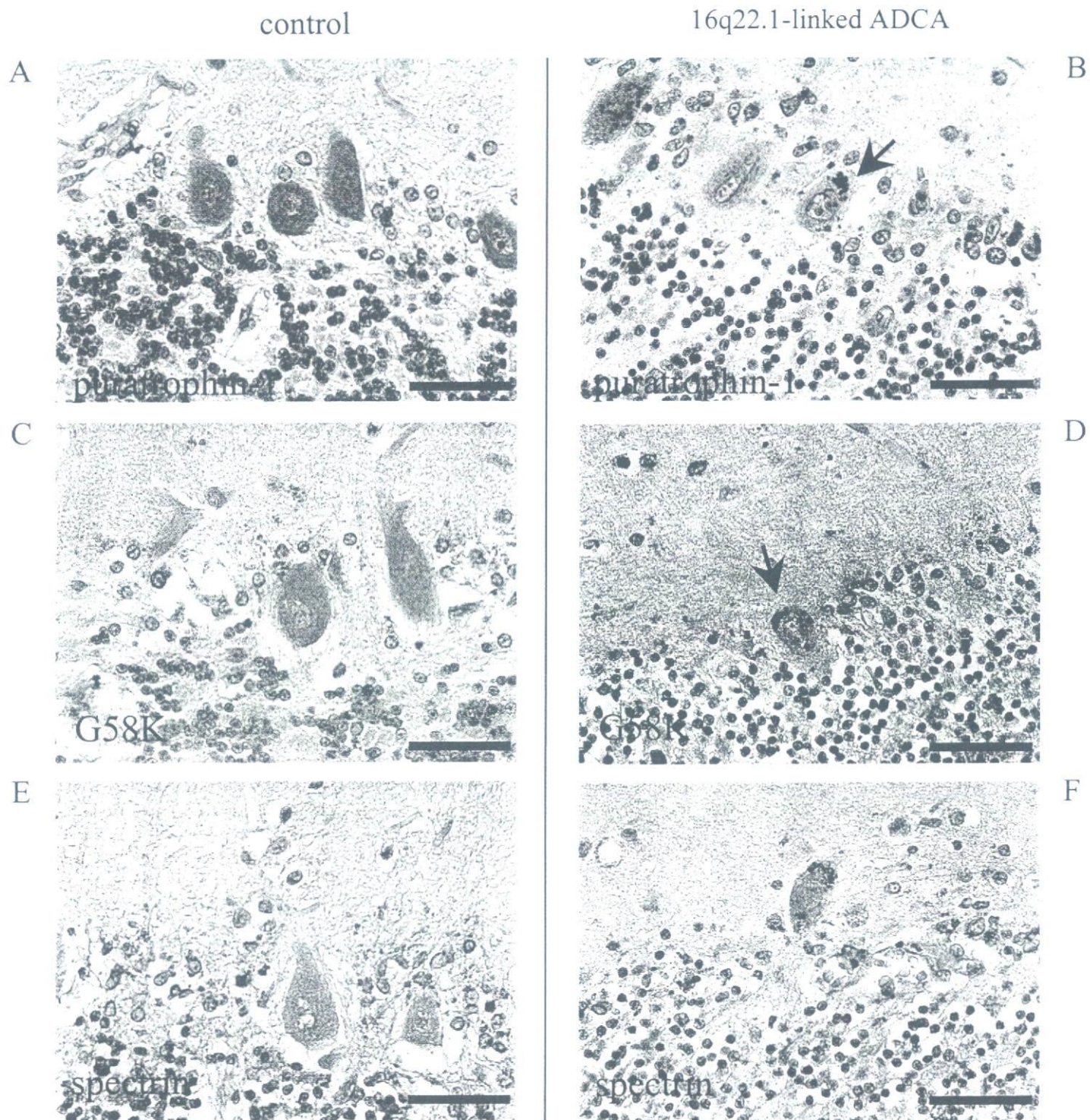
Figure 9 Immunohistochemical analysis of puratrophin-1, Golgi-apparatus membrane protein (G58K), and spectrin in control cells and samples from a patient's cerebellum. *A,* Puratrophin-1 expression in the cell body of Purkinje cells, visualized with use of rabbit polyclonal anti–puratrophin-1 antibody (FL01). *B,* With use of same antibody FL01, aggregation of puratrophin-1 (*arrow*), seen in a Purkinje cell of a brain affected with chromosome 16q22.1–linked ADCA. *C,* G58K expression, seen diffusely in the cell body of control Purkinje cells. *D,* G58K aggregation (*arrow*), morphologically quite similar to the puratrophin-1 aggregate, seen in a patient's Purkinje cell. *E,* Spectrin expression, seen in the cell body of a control Purkinje cell. *F,* Spectrin aggregation in a patient's Purkinje cell. All scale bars = 50 μm.